First principles theory of artificial metal chains on NiAl(110) surface

Arrigo Calzolari[1] and Marco Buongiorno Nardelli[2]
[1]*INFM-S3—National Research Center on nanoStructures and Biosystems at Surfaces, and Dipartimento di Fisica Università di Modena e Reggio Emilia, I-41100 Modena, Italy*
[2]*Center for High Performance Simulations (CHiPS) and Department of Physics, North Carolina State University, Raleigh, North Carolina 27695, USA and CCS-CSM, Oak Ridge National Laboratory, Oak Ridge, Tennessee 37831, USA*
(Received 8 February 2005; revised manuscript received 26 April 2005; published 8 July 2005)

Using first-principle calculations we have studied the stable phases of metal-atom chains on the (110) surface of NiAl. Our investigation is mainly focused on the technologically relevant case of Au chains, but the results will be analyzed in the broader framework of a family of metallic systems. We demonstrate that the nature of the adatom (Au, Mn, Ni, Cu, Al, H, C, Na, K, and Ca) is responsible for different levels of interaction with the substrate and gives rise to a variety of electronic behaviors. With some transition metals (such as Au, Mn, Ni, and Cu) the NiAl surface acts as a simple structural template for the formation of the artificial one-dimensional system and does not affect the electronic properties of the chains. With other atomic species (H, C, Na, K, and Ca) we observe substantially different couplings and stronger interactions. We demonstrate that the different electronic properties of the various adatoms are responsible for different couplings with the substrate and compare our findings with the existing experimental results. Finally, in the case of Au chains we have investigated the role of adatom-adatom interactions in the formation of such one-dimensional structures.

DOI: 10.1103/PhysRevB.72.045416 PACS number(s): 71.15.Ap, 72.10.−d, 73.63.−b

I. INTRODUCTION

The last decade has seen an ever-increasing demand for the design of devices of superior and revolutionary performance that has fueled both basic and applied research at the nanoscale. In this respect, the individual positioning of molecules and even atoms in precise locations of a device is becoming one of the frontiers for nanotechnology. Although still at a prototypical stage, the atom-by-atom fabrication of nanostructures is rapidly becoming a technique of choice for the study of the properties of materials of low-dimensionality and atomic-scale dimensions.

From an experimental point of view several attempts have been made to produce truly one-dimensional (1D) wires at the atomic scale. For instance, following the seminal works by van Ruitenbeek and Takayanagi,[1–3] suspended metallic chains of heavy transition metals (especially Au and Pt[4–9]), were fabricated using mechanically controllable break junctions (MCBJ). The joint application of high resolution transmission electron microscopy (HRTEM) and scanning tunneling/atomic force microscopy[10] (STM/AFM) allowed the investigation of the electronic and transport properties of these chains, which show in the conductance spectra the discontinuous plateaus of conductance quanta typical of one-dimensional systems. However, the existence of quantitative discrepancies among measured *I-V* characteristics suggests a strong correlation between the electronic and the structural properties of the systems. In fact, the MCBJ techniques does not allow the control *in situ* of the single atoms of the chain, and different structural arrangements can be obtained under similar experimental conditions. Several theoretical analysis[11–15] have been proposed to interpret the experimental results.

An alternative approach consists in the formation of long and ordered chains on metal and semiconductors surfaces. The fabrication and characterization of mono-atomic Au chains on various substrates has been the subject of a large body of experimental work.[16–24] The role of the substrate is to act as the template for the assembling of the atomic chain. Along these lines, Ho and co-workers demonstrated[20–23] that it is possible to assemble long gold chains, depositing with a STM tip single Au atoms onto a metallic NiAl(110) surface. The final wires are highly ordered and stable against atomic relaxation, they are frustrated to the NiAl lattice periodicity and show true metallic electronic properties in 1D.

In this paper we will concentrate on monoatomic chains of Au atoms on a substrate of NiAl. In a previous work we studied the transport properties of Au chains upon the adsorption of carbon monoxide molecule.[25] Here we will focus on the intrinsic properties of the chain-surface interface. We will present a comprehensive study of the structural and electronic properties of this system and we will compare our findings with the behavior of mono-atomic chains of other atomic species. In particular, we will discuss the interplay between the nature of the adatom (besides Au we will consider Mn, Ni, Cu, Al, C, H, Na, K, and Ca) and the variety of electronic behaviors that arise from the different levels of interaction with the substrate. We will see that the role of the substrate ranges from a simple structural template for the formation of the artificial one-dimensional system to the formation of adatom-induced surface structures.

The paper is structured as follows: In Sec. II we briefly describe the method. In Sec. III we report our results: The properties of the clean NiAl(110) in Sec. III A; the infinite Au chains adsorbed on NiAl surface in Sec. III B, while in Sec. III C we study the chain-to-surface interaction varying the chemical species of the adatoms. The early stage of the Au chain formation will be discussed for finite ad-structures (atom, dimer, short chain) in Sec. III D.

II. METHOD

We performed state-of-the-art electronic structure calculations[26] based on density functional theory (DFT),[27] with PBE (Ref. 28) generalized gradient approximation for the exchange-correlation functional. The electron-ion interaction was described consistently by *ab initio* ultrasoft pseudopotentials.[29] For a more accurate description of the atomic interactions, we have included the semicore $3d$ ($5d$) shell of Ni (Au) in the valence shell. Semicore shells were also included in the pseudopotentials of other adatoms (e.g., $3d$ in Cu and Mn, and $3s3p$ in K, Ca, and Mn). In the case of Na the interactions with inner electrons were included via nonlinear core corrections.[30]

The infinite surface was simulated by large supercells, where we have included a thick vacuum layer ($\sim$15 Å) in the directions perpendicular to the surface to prevent spurious interactions between adjacent replicas. The number of layers and of adatoms in the unit cell varies, depending on the particular system studied. For infinite chains, the supercell contains five layers of metal alloy with 1×2 periodicity and 1 adatom. In the case of finite structures each slab contains three layers of NiAl(110) with 8×2 periodicity, and one, two, or seven atoms to simulate single adatom, dimer, and seven-atom-long chain structures, respectively. We tested that the reduction of the substrate thickness to 3 layers does not affect significantly the accuracy of the results. For Brillouin zone (BZ) integrations we used 4 (1) special **k** points in the irreducible wedge of the two-dimensional (2D) BZ of the 1×2 (8×2) surface cell. Finally, all structures were relaxed until forces on all atoms were lower than 0.03 eV/Å.

We calculated the STM images within the Tersoff-Hamman approximations[31] under constant current conditions and a negative bias voltage of −400 meV. Consequently, we are scanning the valence states in an energy region around the Fermi level.

III. RESULTS AND DISCUSSION

A. Clean surface

Promising technological applications, e.g., in catalyst reactions and in the aerospace field have motivated extensive studies of the physical properties of NiAl both from an experimental[32–37] and a theoretical[38–41] point of view. Here, we will briefly summarize our results for the structural and electronic properties of the NiAl(110) surface that we will use as common substrate for the formation of monoatomic chains.

NiAl is an alloy that crystallize in the CsCl structure, with 2 inequivalent atoms (Ni and Al) per unit cell and a theoretical lattice parameter a_0=2.94 Å in good agreement with the experimental value (2.89 Å). Figure 1 shows the schematic model of the (110) surface.

The ideal cleavage surface undergoes a structural relaxation, which mainly involves the atoms of the first layer, as summarized in Table I. In the optimized structure we observe a vertical displacement (Δz_{R_1}) of Al and Ni atoms: Outward for Al and inward for Ni, in agreement with experiments[32]

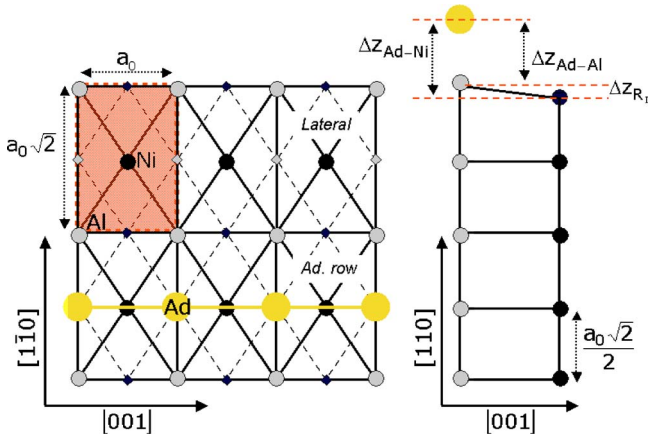

FIG. 1. (Color online) Schematic top (left) and side (right) views of NiAl(110) surface. Gray, dark blue, and large yellow circles describe Al, Ni, and Au atoms, respectively. The Au adsorption site is indicated (Ad), similar configurations have been adopted for other Ad/NiAl(110) systems. Top view model: The 1×2 cell has been periodically repeated to show the gold chains along the [001] direction. The 1×1 unit cell is indicated by the shaded area. Small diamonds represent the second plane positions. a_0 is the bulk lattice parameter.

and previous calculations.[34] Since the structural modifications are negligible for all other planes beneath (even in the presence of the adatoms), hereafter we will refer only to the relaxation of the first layer.

The nature of the rippling may be interpreted on the basis of the electronic structure of the system. Following Kang and Mele,[39] the bulk of NiAl may be considered as a regular array of Ni atoms embedded in a compressed electron gas, created by the *sp* aluminum valence electrons. As a result, the the strong Ni(d)-Al(p) hybridization causes the filling of the d band of NiAl, which is shifted of $\sim$2 eV towards more negative energies, leaving a depletion of states at the Fermi level.[40]

The surface formation involves a charge redistribution in the first layer that leads the displacement of Ni inwards and Al outwards until an electrostatic neutrality is reached.[38,39]

The electronic structure of the relaxed (110) surface is presented in Fig. 2. The total density of states (DOS) in Fig. 2(a) may be resolved in two principal contributions: The first one corresponds to the main peak centered at $\sim$−2.0 eV below the Fermi energy (thick blue line), which derives from the filled d bands of Ni (as described above). The second is the almost uniform Al *sp* band (dashed red line), which spans the whole energy range and dominates the DOS at the Fermi level.

The *sp* character of the surface electronic states is evident in the simulated STM images, as shown in Fig. 2(b). The image shows a large component around the protruding Al atoms with a weak contribution deriving from the Ni atoms. On the contrary, the d states, well below this energy range, do not contribute to the simulated images. The resulting image correctly reproduces the experimental one.[41,42]

Finally, the calculated value of the work function ϕ =4.8 eV, is in good agreement with the experiments (4.6 eV).[34]

TABLE I. Structural parameters for clean surface and Ad/NiAl(110)-(1×2). Distances are expressed in Å and angles in deg. d_I(Ni-Al) is the atomic Ni-Al distance, ω_I is the in-plane Al-Ni angle along the $[1\bar{1}0]$ direction and Δz_{R_I} is the vertical Al-Ni ripple. See text and Fig. 1 for details. Subscript I refers to atoms of the first layer.

	d_I(Ni-Al)		ω_I		Δz_{R_I}			
	Ad. row	Lateral	Ad. row	Lateral	Ad. row	Lateral	Δz(Ad-Ni)	Δz(Ad-Al)
Clean	2.55	2.55	109.2	109.2	0.18	0.18	⋯	⋯
Au	2.59	2.51	109.6	108.9	0.27	0.18	2.11	1.84
Mn	2.59	2.53	109.1	108.4	0.32	0.27	1.81	1.50
Ni	2.56	2.56	107.9	108.5	0.34	0.22	1.85	1.51
Cu	2.58	2.52	110.0	109.0	0.19	0.18	1.91	1.71
H	2.59	2.50	110.7	109.3	0.08	0.14	0.90	0.81
C	2.60	2.53	108.4	108.1	0.41	0.27	1.03	0.62
Al	2.60	2.50	111.6	109.4	−0.02	0.14	1.97	2.00
Na	2.57	2.51	110.3	109.4	0.06	0.12	2.37	2.30
K	2.56	2.53	110.0	109.3	0.07	0.22	2.87	2.81
Ca	2.58	2.52	110.5	109.5	−0.03	0.14	2.43	2.46

B. Au chains on NiAl(110)

The study of Au chains on NiAl(110) is motivated by the experimental observation[20,21] that such structures, even when made of a few (<10) atoms, present electronic properties typical of 1D periodic crystal. Gold chains along the [001] direction were simulated adding one Au atom in the bridge position on Ni troughs in the (1×2) unit cell, as shown Fig. 1(a). This geometry reproduces the experimental configuration.[20,21]

The relaxed wires are thermodynamically stable. In Table II, we compare the adsorption energy (E_{Ads}) of the chain on the surface and the formation energy of an isolated chain ($E_{\mathrm{Form}}^{\mathrm{Chain}}$) with the same geometry. E_{Ads} is the energy difference between the surface with and without adsorbate

$$E_{\mathrm{Ads}} = E_{\mathrm{Tot}}^{\mathrm{Au/NiAl}} - E_{\mathrm{Tot}}^{\mathrm{NiAl}} - E_{\mathrm{Tot}}^{\mathrm{atom}}, \tag{1}$$

while $E_{\mathrm{Form}}^{\mathrm{Chain}}$ is the energy difference between the isolated chain and the single atom

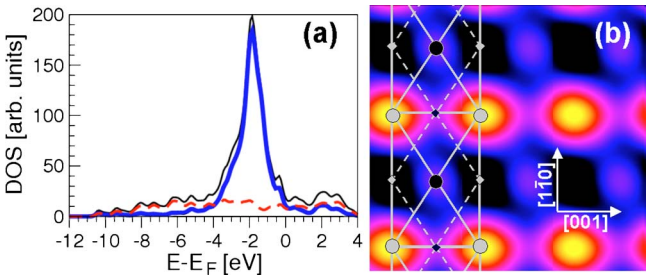

FIG. 2. (Color online) Clean NiAl(110) surface. (a) Total (thin black line) and projected density of states; thick blue and dashed red lines indicate the Ni and Al contribution, respectively. (b) Calculated STM image for clean NiAl(110) surface, obtained at constant current and bias voltage −400 meV. The area corresponding to a 3×2 cell is shown. A schematic atomic structure (as defined in Fig. 1) is superimposed.

$$E_{\mathrm{form}}^{\mathrm{Chain}} = E_{\mathrm{Tot}}^{\mathrm{Chain}} - E_{\mathrm{Tot}}^{\mathrm{atom}} \tag{2}$$

where $E_{\mathrm{Tot}}^{\mathrm{Chain}}$ is the total energy of an isolated chain, calculated in the same unit cell, and $E_{\mathrm{Tot}}^{\mathrm{atom}}$ is the total energy of the adatom [43]. A discrepancy between these two values may indicate the preference of the adatom to bind to the surface or to form chains. From Table II, we observe that the formation of the chain is energetically favored in both cases. However, the difference between the two energies indicates an additional attractive interaction with the substrate, as confirmed also by the reduction of the work function.

The atomic chains are well ordered and do not present structural distortions (e.g., Peierls dimerizations): The presence of the ordered substrate drives the formation of ordered Au wires, where the Au-Au distance (2.93 Å) is induced by

TABLE II. Adsorption energies (E_{Ads}), formation energies of the isolated chain ($E_{\mathrm{Form}}^{\mathrm{Chain}}$) and work functions in different Ad/NiAl(110) systems, All quantities are calculated in eV/Au in the 1×2 unit cell.

	E_{Ads}	$E_{\mathrm{Form}}^{\mathrm{Chain}}$	ϕ(±0.1 eV)
Clean	⋯	⋯	4.8
Au	−2.81	−1.41	4.6
Mn	−4.37	−1.96	4.5
Ni	−4.29	−1.34	4.5
Cu	−3.21	−1.14	4.6
H	−3.60	−0.33	4.8
C	−6.50	−0.98	4.9
Al	−3.52	−1.38	4.6
Na	−1.83	−0.61	3.7
K	−1.14	+0.17	3.5
Ca	−1.88	+0.26	4.0

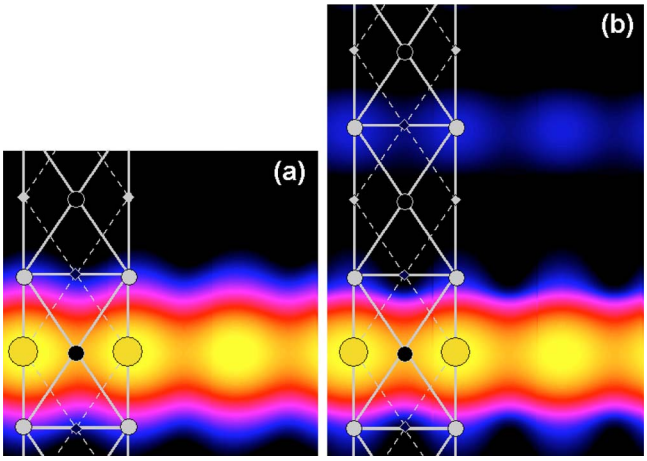

FIG. 3. (Color online) Calculated STM image for Au/NiAl(110) (a) $-\times 2$ and (b) $-\times 3$ surfaces. 1×2 cell has been repeated along [001] direction for clarity. A schematic atomic structure (as defined in Fig. 1) is superimposed.

the Ni-Ni periodicity. The interatomic separation is shorter than in the typical MCBJ experiments under stretching,[1–3] but larger than the DFT equilibrium distance in isolated chains.[11,13,14] Indeed, if we relax the Au-Au distance in chains without the substrate the bond length shrinks down to 2.67 Å (−9%). This geometry would have a formation energy of −1.67 eV/atom, greater than the stretched (2.93 Å) chains, but smaller than in the presence of the substrate (Table II).

Despite the energetic gain in the formation of the chain/surface interface, the overall distortions of the substrate induced by the adatom are small. Table I summarizes the structural parameters (bond length and angles) for the system. We explicitly separate the results regarding the atoms that are nearest-neighbor to the adatoms (labeled "Ad. row"), from those in the adjacent unit cell (labeled "Lateral"), as shown in Fig. 1. The atomic reorganization of the substrate is more appreciable in the unit cell containing the adatom. For instance, the vertical ripple Δz_{R_I} increases beneath the chain ("Ad. row") (with a consequent enhancement of the Ni-Al bonding distortion), but it maintains the same value as the clean surface in the *lateral* cell. The small distortion of the surface close to the adsorption site and its rapid decay along the $[1\bar{1}0]$ direction is the first signature of the one-dimensional (1D) nature of the Au chains.

A similar trend is shown in STM images (Fig. 3): The sequence of spots in the [001] direction represents the chains as observed in STM experiments.[20,21] The STM signal decays rapidly along the $[1\bar{1}0]$ direction. To confirm this finding we simulated the wire in the 1×3 unit cell, i.e., increasing the intra-chain distance. The results are displayed in Fig. 3(b). The absence of Au-Au interaction along the $[1\bar{1}0]$ direction, neither direct nor mediated by the substrate, strengthens the 1D picture of the assembled structures. It confirms also that the $\times 2$ periodicity along the $[1\bar{1}0]$ direction is sufficient to avoid spurious coupling among parallel Au chains.

Nevertheless, to assert that the Au wire on NiAl(110) surface could be considered as an *effective* 1D system (as the isolated one), it is necessary to understand the intrinsic coupling with the substrate and characterize the electronic structure of the Au/NiAl interface.

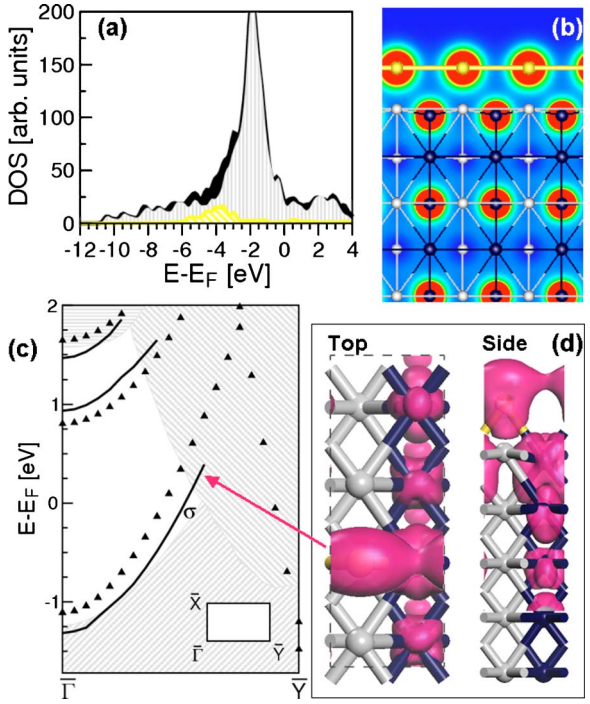

FIG. 4. (Color online) Au/NiAl(110) surface. (a) Total DOS (black area) and projected DOS on Au atoms (yellow area) from Au/NiAl(110) interface; total DOS of clean surface (gray vertical lines). (b) Contour plot of the total charge density in a plane perpendicular to the surfaces containing gold chain and the corresponding Ni row along the [001] direction. Atoms are label as in Fig. 1. The 1×2 cell has been repeated along [001] direction for clarity. (c) Surface band structure along $\bar{\Gamma}$-$\bar{Y}$ direction: Projection of even NiAl (gray area) and Au (black lines) states from Au/NiAl(110) interface, and band structure of isolated Au-chain (triangles). (d) Charge density of a selected state corresponding to the arrow in the band structure.

Our results show that the formation of the gold chain occurs without a remarkable modification of the substrate that acts as an *inert* template for the Au wires and that the total electronic structure of the system results from the simple superposition of the clean surface states and the states of the isolated chain. A first evidence derives from the analysis of the DOS in Fig. 4(a). We compared the total DOS of the surface with (black area) and without (gray vertical lines) the adsorbate. The two plots are almost identical apart from the energy range $\sim[-6,-3]$ eV, where the gold contributions (yellow shaded area) are more evident. The adsorption of the chain happens without the modification of the bonding pattern of the substrate, i.e., without a direct charge sharing between the adsorbate and the alloy, as shown also in the charge density plot of Fig. 4(b).

The DOS component deriving from gold atoms [Fig. 4(a)] may be resolved in two contributions: A localized peak [main contribution to the yellow area in Fig. 4(a)] induced by the fully occupied Au_{3d} states and a dispersive, nondegenerate

σ-band (not appreciable on the scale of the DOS plot), which spans the whole energy spectrum and crosses the Fermi level. These characteristics may be interpreted in terms of the electronic states of an isolated chain, decoupled from the substrate. Due to the low coordination number in the chain, the system looses the spherical symmetry of the bulk, assuming a cylindrical symmetry. From a mathematical point of view, it is possible to label the electronic states of the chain according to the magnetic quantum number m_z. On the basis of symmetry constraints, the d states with $|m_z|=1,2$ remain localized in the narrow peak at lower energy; while the valence Au_{6s} electron ($m_z=0$) hybridizes with the d_0-orbital (the d state with $m_z=0$) leading to high directional σ bonds between neighboring sites.

This behavior is also clear from the electronic band structure of the Au/NiAl interface, plotted in Fig. 4(c). Due to the symmetries of the surface, the electronic states along the $\bar{X}$-$\bar{\Gamma}$-$\bar{Y}$ may be classified as being even or odd with respect to reflection in the mirror plane. Figure 4(c) shows the surface band structure for the *even* states along the $\bar{\Gamma}$-$\bar{Y}$ direction, corresponding to [001] direction in real space. The NiAl contribution to the projected band structure (gray area) does not present significant deviations from the calculated band structure for the clean surface.[34,41] Black lines describe the Au-derived bands: At the Fermi level a σ-like band lies in a pseudo gap of the surface band structure. The depletion of NiAl states justifies the reduced interaction between the Au chain and the substrate.[20,25] The band structure for an isolated Au chain (black triangle), calculated in the same cell, reproduces the main features of the adsorbed one. Outside the internal gaps, the Au-derived bands lose their surface character mixing with the continuum NiAl bulk states. However, the analysis of the Kohn-Sham orbitals does not show a direct coupling between the gold and the surface. As an example, we show in Fig. 4(d) an electronic orbital that results from the noninteracting superposition between the σ-like state stemming from Au-chain and a surface resonance of the substrate.

In summary, the electronic structure at the interface can be outlined as follows: The d components both of the NiAl and of the adsorbate are fully occupied and do not interact at the distances fixed by the geometry. At the Fermi energy, on the contrary, we observe the superposition of the sp states of the substrate, homogeneously distributed on the surface, and the σ-band of gold, oriented along the chain. The absence of surface dangling bonds or of unpaired electrons in the chain does not favor a direct coupling, with shearing or transfer of charge between Au and the substrate. The energy gain mentioned above can be ascribed to electrostatic effects: the quasi-2D electron gas at the surface partially screens the Au-Au interaction, stabilizing the structure at a distance greater than the expected DFT calculations for isolated chains.

On the basis of this discussion, we can re-interpret the bright trace in the STM images (Fig. 3) as the σ-band of the chain, which crosses the Fermi level. The sp orbitals are hidden by the Au states in the "Ad. row" cell, but may be recognized with smaller intensity around the Al atoms (as in the clean surface), along the $[1\bar{1}0]$ direction [Fig. 3(b)]. This feature is the signature of the effective 1D nature of the gold chain on NiAl(110).[25]

C. Comparison with other adatoms

In order to understand the chain/substrate interaction as a function of the adatom electronic structure and to broaden our discussion to other potentially relevant cases, we substituted the Au adatoms with a set of other adsorbates (generally labeled Ad). We considered two class of elements with and without d electrons in the outer valence shell. As prototype of the fist class we chose Mn, Ni, and Cu; while H, C, Al, Na, K, and Ca are representative of the second one. Manganese and Nickel have the $3d$-shell partially occupied; the latter is also one of the constituents of the substrate. Similar to gold, copper has the d shell fully occupied, but it has a smaller covalent radius. Hydrogen and carbon are nonmetallic elements, with very different bonding properties. Aluminum, which is the other component of the alloy, has highly hybridized sp valence electrons. Alkali metals (sodium and potassium) are hydrogenoid metals: The comparison with H and Au allows us to understand the effects of the inner closed shells on the bonding properties of the external s electron, as a function of the covalent radius. Finally, calcium is an example of element with a filled s valence shell.

Not all the Ad/NiAl interfaces that we considered have been experimentally realized. One exception is manganes: In fact the deposition of Mn adatoms or ad-dimers on NiAl(110) has been recently reported.[45,46] A large amount of work has also been devoted to study the adsorption of atomic and molecular hydrogen on NiAl(110) at different coverages.[47–50] In those cases H was not constrained to form 1D chains but was uniformly distributed onto the surfaces. Ad-structures of Ni and Al may be present as defects or steps on the NiAl(110) surface, but generally do not form ordered chains.

For each chemical species, we substituted gold with the new adatom in the same adsorption site (see Fig. 1) and we relaxed the whole structure, in order to obtain adsorbate chains along the [001] directions. The results for the energetics and the optimized geometries are summarized in Tables I and II; while selected STM images are shown in Fig. 5. We observed different regimes: One for transition metal (Mn, Ni, Cu, Au) and Al, one for nonmetals (H, C), and one for akali/alkaline earth (Na, K, Ca).

Transition metals (Mn, Ni, Cu) present characteristics very close to gold. As shown in Table II, we observe a trend going from Mn to Au: As the d shell is filled, the adsorption energy (E_{Ads}) decreases; the work function gets closer to the value of the clean surface while the vertical distances [Δz(Ad-Ni) and Δz(Ad-Al)] increase (see Table I). This fact suggests that the filling of the valence d shell reduces the coupling with the substrate. Similar interpretation derives from the analysis of the electronic structures, that never show the direct formation of chemical bonds between the chain and the substrate. Copper and nickel behaviors are very similar to gold, while manganese seems to be more reactive. In particular, from local spin density (LSD) calculations, the Mn/NiAl(110) interface is spin-polarized with a total mag-

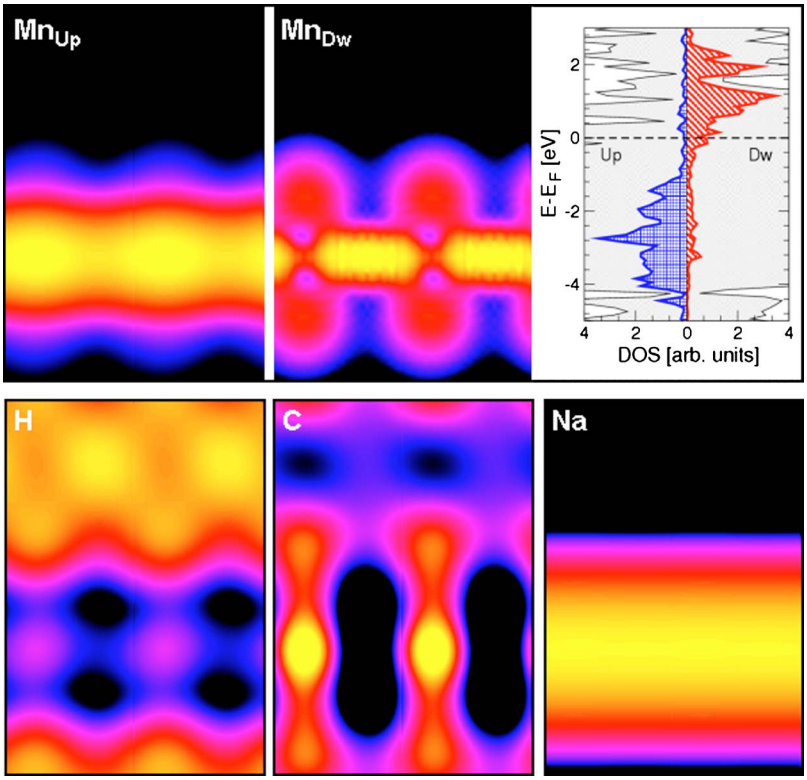

FIG. 5. (Color online) Top panel: Spin polarized STM images and density of states for Mn/NiAl. Total (gray area), and Mn-projected DOS for spin up (squared blue area) and spin down (dashed red area) components. Bottom panel: STM images for selected (H, C, Na) Ad/NiAl(110) structures. 1×2 cell has been repeated along [001] direction for clarity.

netization $\mu_B=4.55$ bohr mag/cell.[51] The spin density (spin up -spin down) is mainly localized around the Mn atoms and extends only slightly to the Ni atoms of the first surface layer. The different electronic structure at the Fermi level modifies the spin-resolved STM images (Fig. 5 top panel). The spin up component shows the hybrid *sd*-band, that characterizes the formation of the 1D gold chain (Fig. 3). On the contrary, spin down image is completely different, with a strong *d* character. The spin up component of DOS (Fig. 5) has the *d* band fully occupied at lower energies and a hybrid σ band that crosses the Fermi level. In the spin down part, the *d* peak is shifted towards the conduction band, and its lowest energy tail characterizes the electronic states at the Fermi level. These spin polarizations are not observed for Ni and Cu, where the overall interface remains nonmagnetic, and the corresponding STM images (not shown here) are identical to the Au case.

This picture changes drastically for the nonmetallic adatoms (H and C), where the direct coupling with the substrate is now favored with respect to the Ad-Ad interaction. Indeed, we observe a great enhancement of the adsorption energy (especially for carbon) and a reduction of the formation energy of the isolated chain (especially for hydrogen). These results are qualitatively in agreement with the experimental observation that the adsorption of hydrogen on NiAl(110) is energetically favored, but it does not form 1D structures.

In both cases, we detect a strong reorganization of the electronic states at the interface and the formation of chemical bonds between the adsorbate and the substrate. However, the adsorption mechanisms of C and H are different. In agreement with experimental results[48] H sits 0.90 Å above the Ni rows (the experimental value is 0.95 Å), and its adsorption locally (Ad. row) removes the ripple relaxation of the clean surface. This behavior is readily understood within a Newns-Anderson model,[52] as originating from the coupling between the localized level of the adsorbate and the broad continuum of states of the substrate. The H_{1s} electron hybridizes with the Ni(*d*)-Al(*p*) band, restoring the charge distribution of the bulk phase. The resulting STM image (Fig. 5) displays a series of maxima, broadly delocalized over the cell, except for the adsorption row. In fact, the formation of the H-Ni bonding states induces a charge depletion around the H adatoms and lowers the energy of the corresponding Ni states, that become inaccessible for the STM detection (at this bias).

In the case of carbon adsorption, the strong hybridization with the surface is coupled with a remarkable distortion of the substrate (Table I), both beneath the adsorption site and in the lateral cell. Carbon binds in bridge position with the two neighboring Al atoms, forming *sp* hybrid orbitals along the $[1\bar{1}0]$ direction. This feature, along with the high C-C distance that does not favor a direct Ad-Ad interaction, prevents the formation of *intrinsic* 1D structures along the [001] direction. The STM images of Fig. 5 confirms this interpretation.

The Al adatoms follow the natural stacking of the surface along the [110] direction. Indeed, the relaxed vertical heights of the adatoms from Ni (1.97 Å) and Al (2.00 Å) of the first layer reproduce the ideal interlayer distance (2.08 Å). Similar to H, Al re-establishes locally the charge distribution of the bulk phase, removing the surface ripple.

For Na, K, and Ca the adsorption energies are much smaller than for the other adatoms, and are even positive in the case of K and Ca. On the other hand, the remarkable reduction of the work function with respect to the clean surface, is a signature of a charge redistribution at the interface.

Similar to hydrogen, the presence of a unique *s* electron in the outer shell does not favor the formation of a highly directional σ bond along the [001] direction. Alkali metals donate their *s* valence electron to the substrate that locally looses the superficial ripple, leaving the adatoms almost ionized. This process leads to an energy gain (E_{Ads}) for the whole interface. On the other hand, because of their large ionic radii, the adatoms sit too close to each other in the geometry induced by the surface periodicity. The electrostatic repulsion between the ions makes the chains thermodynamically unfavorable. We checked this interpretation with two limiting tests: first we relaxed the bonding length in the isolated Na chain, the atom with the smallest radius among the three. The Na-Na equilibrium distance is 3.32 Å, 13% larger than in the constrained configuration. Moreover, we simulated the adsorption of a potassium—the atom with the largest radius—chain onto the (1×3) NiAl(110) surface. The adsorption energy is favored only by 0.1 eV/Au with respect to the chain in the 1×2 unit cell. However, the formation energy of the isolated wire in the 1×3 cell is still positive; hence the main contribution to the electrostatic repulsion stems from the compression of the chain along the [001] direction and only slightly from the intra-chain interaction along the $[1\bar{1}0]$ direction. The corresponding STM images are characterized by a nonstructured bright stripe, delocalized along the the [001] direction, as illustrated in Fig. 5 in the case of sodium.

D. Finite Au structures

In this sections, we focus on the early stages of the Au chain formation, and on the effects induced by the finite-length of the ad-structures on the overall interface.

We studied a single adatom, a dimer and a seven-atom-long wire (labeled Au_7) adsorbed on the NiAl(110) surface. In order to simulate finite ad-structures on a periodic substrate, we used large supercells with 8×2 NiAl(110) periodicity. Starting from the initial states illustrated in Fig. 6(a), we relaxed the three structures. The results for the energetics are summarized in Table III. Table IV reports the parameters for the relaxed geometries. In the case of the single adatom and the dimer, the values are relative only to the atoms close to the adsorption sites: moving away a (1×2) cell from the adsorbates, the surface does not show structural modifications, maintaining the characteristics of the clean surface. Our results are in good agreement with experimental results[20] and with previous DFT investigations for isolated dimers.[54]

As a general trend, we note that going from single atom to the Au_7 wire the interaction with the substrate decreases, assuming the characteristics of the periodic chain described above.

The configuration with the single atom has an adsorption energy[53] 0.12 eV/Au greater than in the infinite chain, denoting a slightly stronger interaction with the substrate. This issue is confirmed by an increase of the structural distortion of the first layer, and by a shorter vertical distance. The atomic *s-d* hybridization, that plays a fundamental role in the formation of Au-Au bonding states in the chain, is ineffective in this case. The 5*d* closed shell does not mix with the 6*s* electron that could interact with the substrate. The adsorbate, not constrained by lateral adatoms, can get closer to the surface and partially hybridize with the *sp* band of the substrate, distorting locally the bonding pattern of the first layer. However, the analysis of the electronic states does not show the formation of bonding states (as seen for H or C), but only a charge polarization at the interface. In agreement with experimental results,[20] the STM image [Fig. 6(b)] shows two contributions: the brightest protrusion centered around the gold metal, and an ordered distribution of spots at lower intensity, that corresponds to the Al *sp* orbitals as in the clean surface [see Fig. 2(b) for comparison].

The inclusion of a second adatom induces an Ad-Ad interaction, not present in the previous case, which competes

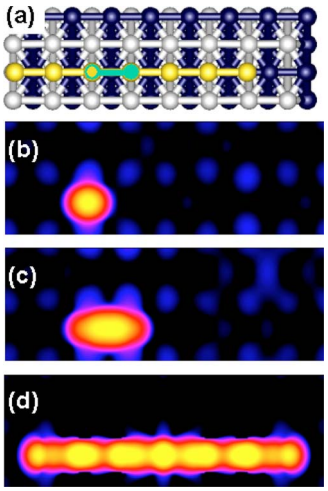

FIG. 6. (Color online) Finite chain structures: (a) Top view of different length (1-2-7) gold structures on NiAl(110)-(8×2) surface. Atoms are labeled as in Fig. 1, green (circled) atoms indicate those employed in the dimer (single adatom) simulations. Calculated STM images for (b) single Au adatom, (c) Au dimer, (d) seven-atom-long Au chain.

TABLE III. Adsorption energies (E_{Ads}), formation energies of the isolated chain ($E_{\mathrm{Form}}^{\mathrm{Chain}}$) in different finite Au structures on NiAl(110)-(8×2) surface.

	E_{Ads} (eV/Au)	$E_{\mathrm{Form}}^{\mathrm{Chain}}$ (eV/atom)
Atom	−2.93	⋯
Dimer	−2.82	−0.96
Au_7	−2.81	−1.34

TABLE IV. Structural parameters for single atoms, dimers and seven-atom-long chains adsorbed on NiAl(110)-(8×2). Distances are expressed in Å and angles in deg. See text for details.

	d_l(Ni-Al)	ω_l	Δz_{R_l}	d(Au-Au)	Δz(Ad-Ni)	Δz(Ad-Al)
Atom	2.66	103.1	0.30	⋯	1.95	1.65
Dimer	2.62	107.0	0.29	2.90	2.03	1.74
Au_7	2.60	109.3	0.28	2.92	2.08	1.80

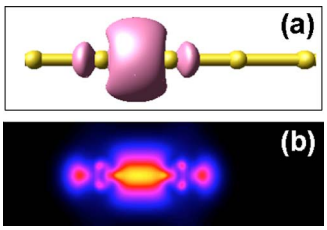

FIG. 7. (Color online) σ-like Wannier function for (a) isolated Au chain and (b) LDOS contour plot obatined from calculated dI/dV STM image for Au dimer on NiAl surface.

with the Ad-surface coupling in the stabilization of the structure. The former interaction seems to rule the process: The two gold atoms bind to each other shearing their valence electrons, but not including the substrate states. The formation of the bond involves also the hybridization with the d electrons. The bond is symmetric and centered between the two atoms, as shown in Fig. 6(c).

Despite the fact that the Au-Au distance is a little frustrated (2.90 Å), the bond has the same characteristics of the periodic chain. We illustrate this finding in Fig. 7, where we compare the Au-Au bonding states calculated for the isolated periodic chain [Fig. 7(a)] and for the Au-Au dimer [Fig. 7(b)] in the presence of the substrate. Figure 7(b) is obtained from a STM simulation in the derivative operating mode (dI/dV) of the whole dimer/NiAl interface. The spectra obtained in this way give a measure of the local density of states (LDOS) at the STM tip apex. Figure 7(a) shows a maximally localized Wannier functions (MLWFs)[55,56] of the isolated chain. Because of their localized character, MLWFs are particulary useful to describe the nature of the chemical bonding.[57] The two panels clearly describe the same bonding σ-state, characteristic of the infinite chains described above. Hence, the key properties of the infinite system are present even in the dimer/NiAl interface.

Extending the length of the wire to seven atoms does not introduce novel features. The structure partially relaxes the stress of the Au-Au bond length, which reaches the value of the periodic wire, except for residual atomic distortions, due to the frustration of the bonds at the boundaries. Following the picture described above, the atomic wavefuctions hybridize and overlap, giving an overall molecular orbital delocalized along the wire. The different intensities of the STM spots [Fig. 6(d)] are the manifestation of the resonance effects on the wave functions, due to the finite size of the Au_7 wire. Passing to the infinite chain these interferences disappear giving the uniform spot distribution of the periodic chain. From an electronic point of view, this implies the extension of the molecular orbitals to the Bloch states, and the formation of 1D σ energy band in the periodic structure.

IV. CONCLUSIONS

In conclusion, we have demonstrated that the formation of linear chains of metal atoms is subordinated to the presence of d electrons in the outer shell of the adatoms, which partially hybridize with the valence s electron, leading to directional σ orbitals, as it is observed in the case of Au, the only system for which these structures have been experimentally observed. In addition, we have related the adatom-to-substrate interaction with the occupation of the d shell: The more it is filled the less is the coupling. The combination of these two properties justifies the appealing effects of the *effective* 1D gold chains on NiAl(110).

ACKNOWLEDGMENTS

We would like to thank A. Ferretti for help and discussions. This work was supported in part by: MIUR (Italy) through grant FIRB-Nomade and by INFM through "Progetto calcolo parallelo." M.B.N. aknowledges the Petroleum Research Fund of the ACS and the Math. Inform. and Comput. Sci. Division, Office of Adv. Sci. Comp. Res. of the U.S. Dept. of Energy under Contract No. DE-AC05-00OR22725 with UT-Battelle and DOE-SC grant "Integrated Multiscale Modeling of Molecular Computing Devices."

[1] A. I. Yanson, G. Rubio Bollinger, H. E. van den Brom, N. Agraït, and J. M. van Ruitenbeek, Nature (London) **395**, 783 (1998).
[2] R. H. M. Smit, Y. Noat, C. Untiedt, N. D. Lang, M. C. van Hemert, and J. M. van Ruitenbeek, Nature (London) **419**, 906 (2002).
[3] H. Ohnishi, Y. Kondo, and K. Takayanagi, Nature (London) **395**, 780 (1998).
[4] S. B. Legoas, D. S. Galvao, V. Rodrigues, and D. Ugarte, Phys. Rev. Lett. **88**, 076105 (2002).
[5] H. Koizumi, Y. Oshima, Y. Kondo, and K. Takayanagi, Ultramicroscopy **88**, 17 (2001).
[6] S. K. Nielsen, K. Hansen, K. Stokbro, J. M. van Ruitenbeek, and F. Besenbacher, Phys. Rev. Lett. **89**, 066804 (2002).
[7] C. Sirvent, J. G. Rodrigo, S. Vieira, L. Jurczyszyn, and F. Flores, Phys. Rev. B **53**, 16086 (1996).
[8] H. Mehrez, A. Wlasenko, B. Larade, J. Taylor, P. Grutter, and H. Guo, Phys. Rev. B **65**, 195419 (2002).
[9] V. Rodrigues, J. Bettini, P. C. Silva, D. Ugarte, Phys. Rev. Lett. **91**, 096801 (2003).
[10] G. Rubio-Bollinger, S. R. Bahn, N. Agraït, K. W. Jacobsen, and S. Vieira, Phys. Rev. Lett. **87**, 026101 (2001).
[11] D. Sanchez-Portal, E. Artacho, J. Junquera, P. Ordejon, A. Garcia, and J. M. Soler, Phys. Rev. Lett. **83**, 3884 (1999).
[12] H. Hakkinen, R. N. Barnet, A. G. Scherbakov, and U. Landman, J. Phys. Chem. **104**, 9063 (2000).
[13] S. R. Bahn and K. W. Jacobsen, Phys. Rev. Lett. **87**, 266101 (2001); and S. R. Bahn, N. Lopez, J. K. Norskov, and K. W. Jacobsen, Phys. Rev. B **66**, 081405(R) (2002).
[14] S. B. Ugarte, D. S. Galvao, V. Rodrigues, and D. Ugarte, Phys. Rev. Lett. **88**, 076105 (2002).
[15] J. J. Palacios, A. Perez-Jimenez, E. Luis, E. SanFabian, and J. A. Verges, Phys. Rev. B **66**, 035322 (2002).

[16] J. N. Crain, A. Kirakosian, K. N. Altman, C. Bromberger, S. C. Erwin, J. L. McChesney, J.-L. Lin, and F. J. Himpsel, Phys. Rev. Lett. **90**, 176805 (2003).
[17] J. N. Crain, J. L. McChesney, F. Zheng, M. C. Gallagher, P. C. Snijders, M. Bissen, C. Gundelach, S. C. Erwin, and F. J. Himpsel, Phys. Rev. B **69**, 125401 (2004).
[18] S. C. Erwin, Phys. Rev. Lett. **91**, 206101 (2003).
[19] J. N. Crain and D. T. Pierce, Science **307**, 703 (2005).
[20] N. Nilius, T. M. Wallis, and W. Ho, Science **297**, 1853 (2002).
[21] T. M. Wallis, N. Nilius, and W. Ho, Phys. Rev. Lett. **89**, 236802 (2002).
[22] N. Nilius, T. M. Wallis, and W. Ho, Phys. Rev. Lett. **90**, 186102 (2003).
[23] G. V. Nazin, X. H. Qiu, and W. Ho, Science **302**, 77 (2003).
[24] N. Nilius, T. M. Wallis, and W. Ho, J. Phys. Chem. B **108**, 14616 (2004).
[25] A. Calzolari, C. Cavazzoni, and M. Buongiorno Nardelli, Phys. Rev. Lett. **93**, 096404 (2004).
[26] Computer code: PWSCF by S. Baroni, A. Dal corso, S. De Gironcoli, and P. Giannozzi, www.pwscf.org.
[27] R. M. Dreizler and E. K. U. Gross, *Density Functional Theory. An approach to the quantum many-body problem* (Springer-Verlag, Berlin 1990).
[28] J. P. Perdew, K. Burke, and M. Ernzerhof, Phys. Rev. Lett. **77**, 3865 (1996); **78**, 1396 (1997).
[29] D. Vanderbilt, Phys. Rev. B **41**, 7892 (1990).
[30] S. G. Louie, S. Froyen, and M. L. Cohen, Phys. Rev. B **26**, 1738 (1982).
[31] J. Tersoff and D. R. Hamman, Phys. Rev. B **31**, 805 (1985).
[32] H. L. Davis and J. R. Noonan, Phys. Rev. Lett. **54**, 566 (1985).
[33] S. M. Yalisove and W. R. Graham, Surf. Sci. **183**, 556 (1987).
[34] S.-C. Lui, M. K. Kang, E. J. Mele, and E. W. Plummer, Phys. Rev. B **39**, 13149 (1989).
[35] M. Wuttig, W. Hoffmann, E. Preuss, R. Franchy, H. Ibach, Y. Chen, M. L. Xu, and S. Y. Tong, Phys. Rev. B **42**, 5443 (1990).
[36] G. R. Castro, H. Dürr, R. Fischer, and Th. Fauster, Phys. Rev. B **45**, 11989 (1992).
[37] K. Gschneidner, Jr., A. Russell, A. Pecharsky, J. Morris, Z. Zhang, T. Lograsso, D. Hsu, C. H. C. Lo, Y. Ye, A. Slager, and D. Kesse, Nat. Mater. **2**, 587 (2003).
[38] J. I. Lee, C. L. Fu, and A. J. Freeman, Phys. Rev. B **36**, 9318 (1987).
[39] M. K. Kang and E. J. Mele, Phys. Rev. B **36**, 7371 (1987).
[40] S.-C. Lui, J. W. Davenport, E. W. Plummer, D. M. Zehner, and G. W. Fernando, Phys. Rev. B **42**, 1582 (1990).
[41] K. Højurp Hansen, J. Gottschalck, L. Petersen, B. Hammer, E. Laegsgaard, F. Besenbacher, and I. Stensgaard, Phys. Rev. B **63**, 115421 (2001).
[42] G. V. Nazin, X. H. Qiu, and W. Ho, Phys. Rev. Lett. **90**, 216110 (2003).
[43] We are well aware of the problems related to the definition of the total energy of a single atom in pseudopotential DFT calculations. However, the choice of bulk energy as a reference for gold is too distant from the experimental configuration. On the other hand, the exact evaluation of this quantities for comparison with experiments goes beyond the aim of this work.
[44] A. Calzolari, N. Marzari, I. Souza, and M. Buongiorno Nardelli, Phys. Rev. B **69**, 035108 (2004).
[45] H. J. Lee, W. Ho, and M. Persson, Phys. Rev. Lett. **92**, 186802 (2004).
[46] A. J. Heinrich, J. A. Gupta, C. P. Lutz, and D. M. Eigler, Science **306**, 466 (2004).
[47] B. Hammer and M. Scheffler, Phys. Rev. Lett. **74**, 3487 (1995).
[48] A. T. Hanbicki, A. P. Baddorf, E. W. Plummer, B. Hammer, and M. Scheffler, Surf. Sci. **331-333**, 811 (1995).
[49] D. Farias, M. Patting, and K. H. Rieder, J. Chem. Phys. **117**, 1797 (2002).
[50] A. T. Hanbicki, P. J. Rous, and E. W. Plummer, Phys. Rev. B **67**, 205405 (2003).
[51] The detailed investigation of the magnetic order (ferro- vs antiferromagnetic) of the interface goes beyond the aim of the present work.
[52] D. M. Newns, Phys. Rev. **178**, 1123 (1969); J. Harris and S. Andersson, Phys. Rev. Lett. **55**, 1583 (1985).
[53] The adsorption energy for finite structures is calculated as in Eq. (1), divided by the number of the adatoms.
[54] N. Nilius, T. M. Wallis, M. Persson, and W. Ho, Phys. Rev. Lett. **90** 196103 (2003).
[55] WanT Code by A. Calzolari, C. Cavazzoni, N. Marzari, and M. Buongiorno Nardelli, www.wannier-transport.org. See also Ref. 44.
[56] N. Marzari and D. Vanderbilt, Phys. Rev. B **56**, 12847 (1997).
[57] S. F. Boys, Rev. Mod. Phys. **32**, 296 (1960).